A case study in applying docking predictions: Modelling the tentoxin binding sites of chloroplast F1-ATPase

Vladimir Sobolev[†,]*, Alidin Niztaev[†], Uri Pick[‡], Adi Avni[#] and Marvin Edelman[†]

[†]Department of Plant Sciences, [‡]Department of Biological Chemistry, Weizmann Institute of Science, Rehovot 76100, Israel
[#]Department of Plant Sciences, Tel Aviv University, Tel Aviv 69978, Israel

The study presents an *ab initio* approach for locating a ligand-binding site and demonstrates that relevant conclusions can be deduced from multiple, predicted ligand positions. Tentoxin is a specific inhibitor of plastid CF1-ATPase, its interaction with the α- and β-subunits of the enzyme resulting in complex interference with ATPase activity. The uniquely different conformations of the β-subunits in the quasi-symmetrical structure of the F1-ATPase from bovine mitochondria offer an opportunity to model tentoxin binding at multiple sites in plastid CF1-ATPase. Using software for molecular docking, we located and analysed three putative binding sites with approximately equally high complementarity to tentoxin. Complementarity at these sites is sensitive to the nucleotide occupancy state of the β-subunit. The main interactions stabilizing the putative complexes were determined, and homology models for the tentoxin-binding sites of *Chlamydomonas* plastid CF1-ATPase were created. The predicted binding pocket residues for Site I are at the α_{TP}/β_{TP} interface and include residue Glu-67β_{TP} (codon 83β in plastid CF1-ATPase), previously identified as a molecular-genetic determinant for the high affinity, inhibitory response to tentoxin in *Chlamydomonas*. This site overlaps with that suggested by others, but ~50% of residues differ. Sites II and III, possibly related to low-affinity binding of tentoxin, are located in functionally active regions: one entirely within the α_{TP}-subunit and sharing a residue with the α_{TP} nucleotide-binding site; the other at the $\alpha_{TP}/\beta_E/\gamma$ interface and sharing a residue with the conserved DELSEED sequence. Non-catalytic residues in these putative pockets represent potential targets for mutational analysis.

ANY molecular docking approach trying to predict the structure of a protein–ligand complex faces three major problems: locating the approximate position of the binding site, generating a computationally sufficient number of ligand positions within the binding site, and defining the most probable position for the ligand. Molecular biologists are mainly interested in answering the last point in order to analyse interactions that stabilize the complex. This analysis permits them to predict desired modifications of the ligand (ligand design) and/or protein (protein engineering) in order to regulate the binding. In many, but not all cases, researchers can rely on external experimental information for locating the ligand-binding site. In addition, established docking procedures exist for generating and scoring ligand positions within a presumptive binding site, but in most cases several positions appear to have the same probability. In this study, we present an *ab initio* approach for locating a binding site and demonstrate that relevant conclusions can be deduced from multiple, predicted ligand positions.

F_0F_1-ATPase (ATP synthase) is a central enzyme in energy conversion in chloroplasts, mitochondria and bacteria. The main reaction catalysed by this enzyme is ATP

formation from ADP and Pi, using energy derived from a transmembrane electrochemical potential gradient. In chloroplasts, a transmembrane electrochemical proton potential difference is built up by photosynthetic electron transport. The soluble part of the proton ATPase (F1 in mitochondria and CF1 in chloroplasts) in the isolated form catalyses the reverse reaction, ATP hydrolysis. The activity of F1 or CF1, both in the forward and backward direction, may be perturbed by specific inhibitors or activators[1]. Among well-studied examples are complexes of bovine mitochondrial F1-ATPase with aurovertin, efrapeptin, nitrozobenzofurazan, dicyclohexylcarbodiimide and non-hydrolysable ATP analogues[2–5]. Clarification of the interaction of highly specific inhibitors with CF1 or F1 offers a powerful means to unravel the complex structural dynamics associated with ATP formation.

Tentoxin (cyclo-[L-leucyl-*N*-methyl-(Z)-dehydrophenylalanyl-glycyl-*N*-methyl-alanyl]), a naturally-occurring tetrapeptide[6], affects chloroplast CF1-ATPase activity[7] of sensitive plant species[8] in a biphasic manner. Non-competitively[9], it inhibits ATP hydrolysis and photophosphorylation[10] at low concentrations (10^{-8} to 10^{-7} M), while stimulating ATP hydrolysis at higher concentrations (10^{-5} to 10^{-4} M)[9,11]. The stimulatory effect has been observed in isolated CF1, in thylakoid membranes, and in

*For correspondence. (e-mail: vladimir.sobolev@weizmann.ac.il)

reconstituted proteoliposomes[12]. Tentoxin has not been found to inhibit mitochondrial or bacterial ATPase and does not inhibit plastid ATPase of tentoxin-resistant photosynthetic species. Therefore, tentoxin may be utilized to analyse subtle structural differences in catalytic domains of the enzyme.

The mechanism of tentoxin inhibition and reactivation is not well understood and the number of binding sites involved is controversial. Equilibrium dialysis with synthetic tentoxin analogues[13] and radiolabelled tentoxin[14] revealed two binding sites with high and low affinities, that were correlated with the inhibitory and stimulatory effects respectively. The existence of a third, very-low-affinity binding site that could account for the stimulatory effect has also been suggested[15]. In early studies, the inhibitory, high-affinity site of tentoxin was localized to the α- and β-subunits of CF1[16]. More recently, Avni et al.[17] identified codon 83 of the β-subunit as a specific site which confers differential sensitivity to tentoxin in the genus Nicotiana. This conclusion was substantiated by mutagenesis of the corresponding site in the tentoxin-insensitive, transformable green alga Chlamydomonas[17,18] and in the Rhodospirillum rubrum chromatophore reconstitution system[19]. Thus, the 83β site offers a natural starting point in the search for high-affinity binding pocket. The location(s) of the low affinity site(s), however, is more obscure. On the basis of kinetic and equilibrium experiments, an interaction of the low affinity site with the nucleotide-binding sites has recently been proposed[14], involving a complex relationship between the catalytic state and tentoxin-induced F1-ATPase stimulation. An alternate proposal, based on heterologous chromatophore reconstitution experiments, implicates codon 83β in the low, as well as high, affinity site[20].

A perusal of the protein database (PDB)[21] using LPC software[22] readily reveals that a ligand of the size of tentoxin invariably contacts multiple residues. Thus, a structural analysis of the tentoxin-binding sites could add considerably to the existing molecular–genetic and biochemical studies and deepen our understanding of the mechanism by which the toxin inhibits or stimulates chloroplast CF1-ATPase. The structures of mitochondrial[2–5,23,24] bacterial[25] and chloroplast[26] F1-ATPase have been reported. The structure of the $\alpha_3\beta_3\gamma$ complex of F1-ATPase from bovine heart mitochondria[23] shows that the three catalytic β-subunits differ in conformation and occupancy of the nucleotide-binding site. The structures of the nucleotide-free $\alpha_3\beta_3\gamma\epsilon$ complex from chloroplast CF1-ATPase of spinach[26] and $\alpha_3\beta_3$ complex of F1-ATPase from the thermophilic Bacillus PS3[25] were determined by molecular replacement based on the structure of the bovine mitochondrial enzyme. The $\alpha_3\beta_3\gamma$ complex of F1-ATPase from rat liver mitochondria has all catalytic and non-catalytic sites occupied with nucleotide[24]. In all these studies, the overall structure and sequence

of the catalytic α- and β-subunits are highly similar. Indeed, the primary sequences of mitochondrial and chloroplast α- and β-subunits are respectively, ~55 and 70% identical. In particular, a BLAST-P[27] scan of non-redundant F1-ATPase β-subunit sequences from plastids, mitochondria and bacteria reveals >100 files, all of which contain a conserved negative charge at the 83β site.

We have chosen to model the binding site(s) of tentoxin to CF1-ATPase based on the structure of the F1-ATPase from bovine heart mitochondria. The uniquely different conformations of the β-subunits in this quasi-symmetrical structure[23] offer an opportunity to model tentoxin-binding at multiple sites in CF1-ATPase. In this study, we search for theoretical binding sites of the toxin and model the consequences of complex formation. We dock the toxin in the resolved structures, predict the main stabilizing interactions of the resulting putative complexes, and create homology models for the tentoxin-binding site(s) of Chlamydomonas plastid CF1-ATPase.

Recently, Groth[28] has resolved the structure of spinach CF1-ATPase complexed with tentoxin to a resolution of 3.4 Å. The crystal structure confirms the general location of the high-affinity binding site in the codon 83β pocket, but the weak and averaged electron density did not allow an accurate pinpointing of the inhibitor. The docking data presented by our predictive methodology seem more relevant as regards the geometry of the ligand, the absence of ligand–protein bumping, and the fitting to the shape of the cavities. Interestingly, the fitting found by us at the codon 83β site is significantly shifted towards the α-subunit, in agreement with other biochemical data. Importantly, our predictions, based on the quasi symmetrical bovine mitochondrial structure, contain original assumptions on the location of low-affinity binding sites in catalytic zones of the complex. These sites were not resolved in the crystal structure of the nucleotide-free CF1-tentoxin complex.

Results

Probe cavities and ligand docking

The entire structure (minus water molecules) of the bovine mitochondrial crystal of the PDB file 1cow was pre-scanned with a probe molecule consisting of the tentoxin ring without methyl-dehydrophenylalanyl and methyl-alanyl side chains. This procedure enabled us to avoid considering ligand side-chain orientations and to retain tight pockets. Since the volume and shape of the ring depended slightly on its conformation, we used only the prevalent A-conformer[29]. In essence, the scan searched for cavities into which the backbone ring of tentoxin could fit sterically. Scanning was performed

using LIGIN[30] and assuming all ligand atoms as neutral. The various approximations reduced the time required for docking the probe molecule vs tentoxin itself by ~ 250-fold. The three-dimensional space of the 1cow $\alpha_3\beta_3\gamma$ crystal was divided into ~ 1500 cubes, and the probe was docked in each. Only probe positions separated by 5 Å or more were tallied. The resulting list of cavities, in decreasing order of complementarity, contained 837 members, including those completely burying the probe molecule as well as some with only a few probe atoms in contact with the protein.

We docked all 22 conformations (see the section on 'Materials and methods') of tentoxin into the 230 highest-scoring probe cavities. For each cavity, the docked conformation yielding the highest complementarity value was scored. A small number (3%) of scored structures were discarded due to ligand–protein bumping. Those remaining, ranged in complementarity values from 454 to 226 Å^2. All docked conformations in the top 10 percentile were analysed. Three unique sites were found: Site I (probe-cavity 5; complementarity to tentoxin, 445 Å^2), formed by α_{TP}- and β_{TP}-subunits; Site II (probe-cavity 22; complementarity, 437 Å^2), formed by α_{TP}-subunit alone; Site III (probe-cavity 59; complementarity, 454 Å^2), formed by α_{TP}, β_E and γ. All other structures in the top ten percentile range were lower value variants of Site III. Putative sites in the next ten percentile range were of lower complementarity and are not presented here. (Their location and LPC analysis can be found at http://sgedg.weizmann.ac.il/tentoxin/).

A set of residues forming a binding site is composed of those residues that are in contact with tentoxin in at least one of the 22 conformations docked at that site. The set of residues forming Site I is listed in the leftmost column of Figure 1 e, while the set of residues forming Site II is: α_{TP} (A152, L156, E353, E355, L356, K359, I361, P363, I365, N366, V367, G368, L369, L394, Y397, R398, A401, A402, F403, V422, T425, L428); and that forming Site III is: α_{TP} (F406, S408), β_E (S383, D386, I387, I390, L391, E395) and γ (K24, M25, A28, Y31, A32, E35, M229, T230, D233, N234, K237). Sites I and II take the form of pockets in which the ~ 600 Å^2 surface of the tentoxin molecule is ~ 90% complexed with the protein. Site III forms a niche in which the toxin molecule fits with high complementarity, but remains ~ 40% surface-exposed.

The predicted positions having the highest complementarity for each ring form of tentoxin at Site I are displayed in Figure 1. Site I, which includes E67β_{TP} (CF1 codon 83β), is spacious, the ligand contacting somewhat different subsets of residues in each case (Figure 1 a–d). Those residues common to all the four ring structures (Figure 1 e) are the most probable to be in contact with tentoxin at this site. The schematic locations of Sites I, II and III within the $\alpha_3\beta_3\gamma$ crystal structure are shown in Figure 2.

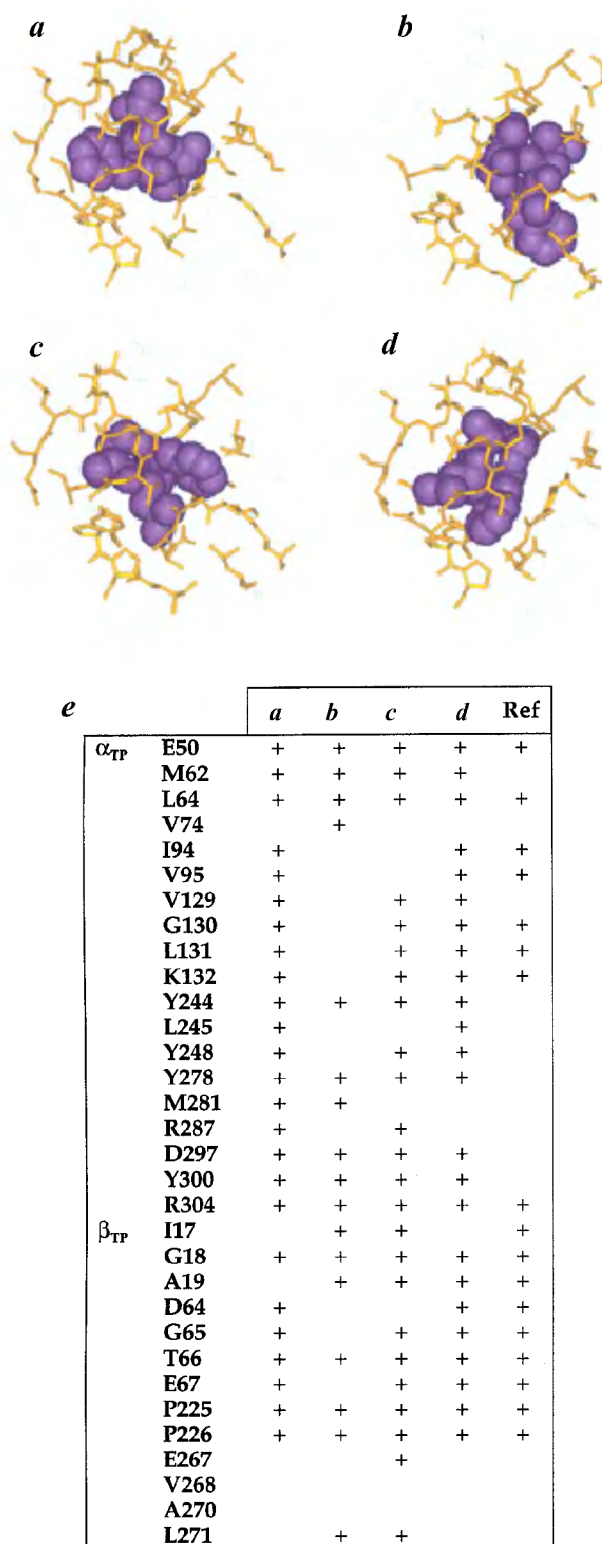| e		a	b	c	d	Ref
α_{TP}	E50	+	+	+	+	+
	M62	+	+	+	+	
	L64	+	+	+	+	+
	V74		+			
	I94	+			+	+
	V95	+			+	+
	V129	+		+	+	
	G130	+		+	+	+
	L131	+		+	+	+
	K132	+		+	+	+
	Y244	+	+	+	+	
	L245	+			+	
	Y248	+		+	+	
	Y278	+	+	+	+	
	M281	+	+			
	R287	+		+		
	D297	+	+	+	+	
	Y300	+	+	+	+	
	R304	+	+	+	+	+
β_{TP}	I17		+	+		+
	G18	+	+	+	+	+
	A19		+	+	+	+
	D64	+			+	+
	G65	+		+	+	+
	T66	+	+	+	+	+
	E67	+		+	+	+
	P225	+	+	+	+	+
	P226	+	+	+	+	+
	E267			+		
	V268					
	A270					
	L271		+	+		

Figure 1. Predicted positions for tentoxin at Site I. *a–d*, Modelled structure with the highest complementarity for each ring conformation. Colour code: Purple, tentoxin; brown, residues in contact with tentoxin; green, Site I residues not in contact with tentoxin in the given ring form. *e*, Complete list of residues forming Site I. For each position of tentoxin shown, the contacting residues are marked. The rightmost column (Ref) lists residues from Groth and Pohl[26] that overlap with Site I. Molecular graphics were created using InsightII software (MSI, Inc.).
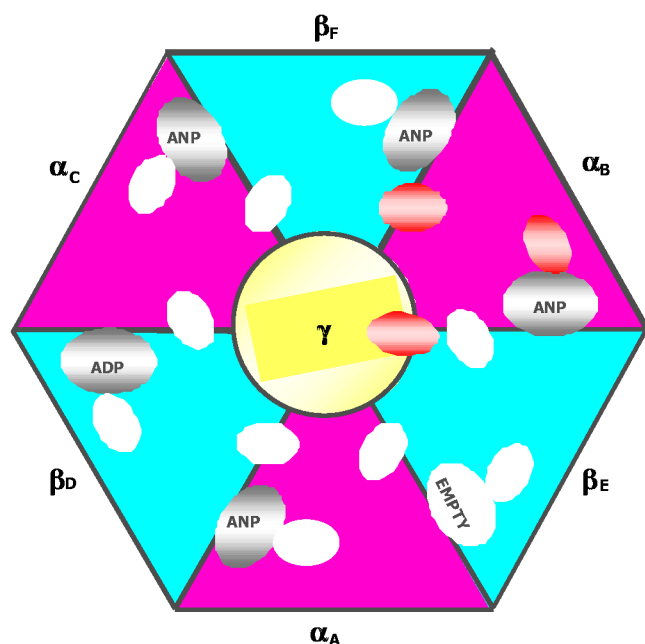
Figure 2. Schematic presentation of the $\alpha_3\beta_3\gamma$ complex (PDB file 1bmf), with four ANP (adenylyl-imidodiphosphate), one ADP and one empty nucleotide-binding site. The hypothetical tentoxin-binding sites are shown. Site I, formed by the α_{TP}/β_{TP} interface has 'sister' cavities at the α_{DP}/β_{DP} and α_E/β_E interfaces. Site II, in the α_{TP}-subunit, has 'sister' cavities in subunits α_E and α_{DP}. There are, altogether, an additional six counterpoint cavities (drawn but not marked) which emanate from similarities in sequence and overall structure between the α- and β-subunits. Site III is located at the $\alpha_{TP}/\beta_E/\gamma$ interface.

Symmetries in F1-ATPase

Due to the quasi 3-fold symmetry of the bovine $\alpha_3\beta_3\gamma$ structure[23], Sites I and II each have two additional 'sister' cavities – for Site I, at the α_{DP}/β_{DP} and α_E/β_E interfaces, and for Site II, in the α_E- and α_{DP}-subunits (Figure 2). The complementarities of tentoxin to these cavities are less than those to the putative pockets (Table 1). A further level of symmetry, arising from partial homology[31] and similar folding topologies[2] of α- and β-subunits, adds a set of counterpoint cavities to Sites I and II (cf., Figure 2). The highest complementarity to tentoxin among these is for cavities at the β_{DP}/α_E interface (382 Å^2) and in the β_{TP}-subunit (349 Å^2). The counterpoint cavities are considerably less fit as potential toxin-binding sites than Sites I and II. Site III, which interfaces partially with the unique γ-subunit, does not have additional counterparts in the crystal structure. However, it is likely that during functional rotation[32,33] complementary cavities do form at the various $\alpha/\beta/\gamma$ interfaces.

Tentoxin binding in quasi-symmetrical cavities

Docking of tentoxin at each of the three Site I interfaces (α_{TP}/β_{TP}, α_{DP}/β_{DP} and α_E/β_E) revealed different comple-

mentarities (Table 1). Consequently, the three Site I pockets are not identical. To measure their differences, we superimposed all backbone and side chain atoms of the residues forming the sites. The results showed that the interface cavity of α_E/β_E differs from that of α_{DP}/β_{DP} by a relatively small degree (RMSD = 0.81 Å for backbone atoms and 0.91 Å for backbone plus side chain atoms), while the same α_{TP}/β_{TP} cavity differs from that of α_E/β_E by a larger amount (RMSD = 1.78 Å for backbone atoms and 1.96 Å for backbone plus side chain atoms). Thus, the inherent flexibility of the $\alpha_3\beta_3\gamma$ molecule[23,34–36] is manifested also by measurement of the Site I region. A second major conclusion from Table 1 is that for all four tentoxin ring structures analysed, Site I at the α_{TP}/β_{TP} interface has the highest complementarity and, consequently, the highest probability to be occupied. In contrast, Site I at the α_E/β_E cavity has the lowest complementarity and, therefore, the lowest probability to be occupied.

Docking tentoxin into the symmetrical Site II cavities of α_E-, α_{TP}- and α_{DP}-subunits also produced different complementarities (Table 1). The main conclusion drawn is that the cavity formed in the α_{DP}-subunit has the lowest probability to be occupied by tentoxin, while the remaining two Site II cavities are occupied with approximately the same probability. Site II in the α_{TP}-subunit is favoured since it shows the highest complementarity (437 Å^2 for ring conformation B; Table 1).

As already noted, Site III is formed in part by residues of the unique γ-subunit and, therefore, lacks quasi-symmetry at the five other interfaces of the $\alpha_3\beta_3\gamma$ lattice. The highest complementarity (454 Å^2) is for the B-form of the tentoxin ring (Table 1).

Applying the modelling results to CF1-ATPase

The conclusions drawn from modelling binding sites for tentoxin in F1-ATPase were applied to modelling the analogous sites in CF1-ATPase. The amino acid sequences of the α-, β- and γ-subunits of F1- and CF1-ATPase from bovine mitochondria and the chloroplast of *Chlamydomonas* were aligned (Figure 3) and compared with regard to their respective, putative tentoxin-binding site residues. Site I residues (located in α_{TP}- and β_{TP}-subunits) are highlighted in yellow. Site II residues (located solely in the α_{TP}-subunit) are highlighted in cyan. Site III residues (located in α_{TP}-, β_E- and γ-subunits) are highlighted in green. The degree of matched F1 and CF1 residues at the three binding sites matched the general level of homology for the relevant subunits of the two ATPases.

The main interactions stabilizing complex formation with tentoxin were analysed. Table 2 lists the relevant residues in the mitochondrial and chloroplast subunits for Site I. Putative hydrogen bonds, or hydrophobic–

Table 1. Complementarity (Å^2) of tentoxin at docked binding sites[a]

Tentoxin ring conformation	Site I			Site II			Site III
	α_{TP}/β_{TP}	α_{DP}/β_{DP}	α_E/β_E	α_E	α_{TP}	α_{DP}	$\alpha_{TP}/\beta_E/\gamma$
A	**445**	345	241	390	362	306	421
B	414	296	195	386	**437**	306	**454**
C	408	286	146	356	357	331	416
D	443	301	255	392	399	338	414

[a]Bold numbers indicate the highest complementarity for the site.

Table 2. Site I residues at the α_{TP}/β_{TP} interface forming potential hydrogen bonds or hydrophobic contacts with tentoxin

Bovine mitochondria	Subunit	Tentoxin ring conformation[a]				*Chlamydomonas* chloroplast[b]
		A	B	C	D	
Potential hydrogen bonds						
Glu-50	α_{TP}	+	−	+	+	Gly-51
Tyr-244	α_{TP}	+	+	+	+	Tyr-237
Tyr-278	α_{TP}	+	+	−	−	Tyr-271
Tyr-300	α_{TP}	−	−	+	+	Tyr-293
Arg-304	α_{TP}	+	+	+	+	Arg-297
Thr-66	β_{TP}	−	+	+	−	Thr-82
Potential hydrophobic contacts						
Met-62	α_{TP}	+	+	+	−	Ile-63
Leu-64	α_{TP}	+	+	+	−	Leu-65
Ile-94	α_{TP}	+	+	−	+	Ile-95
Val-95	α_{TP}	+	+	−	+	Ala-96
Val-129	α_{TP}	+	+	−	+	Ile-130
Tyr-244	α_{TP}	+	+	−	+	Tyr-237
Leu-245	α_{TP}	+	+	−	+	Leu-238
Tyr-248	α_{TP}	+	+	−	+	Tyr-241
Tyr-300	α_{TP}	−	−	+	+	Tyr-293
Ala-19	β_{TP}	−	+	+	+	Pro-29
Thr-66	β_{TP}	−	+	−	+	Thr-82
Pro-225	β_{TP}	+	+	+	+	Pro-242
Pro-226	β_{TP}	+	+	+	+	Pro-243
Leu-271	β_{TP}	−	+	+	−	Leu-288

[a]For each ring conformation, analysis was performed for the complexed structure with the highest complementarity.
[b]As aligned in Figure 3 *a* and *b*.

hydrophobic contacts, are listed only when two or more ring conformations scored positive. Tyr-244α_{TP} and Arg-304α_{TP} are predicted to form hydrogen bonds with tentoxin in all ring conformations, while Glu-50α_{TP} will form a hydrogen bond in 3 of 4 cases. Similarly, Pro-225β_{TP} and Pro-226β_{TP} form hydrophobic–hydrophobic contacts with tentoxin in all ring conformations, while Met-62α_{TP}, Leu-64α_{TP}, Ile-94α_{TP}, Val-95α_{TP}, Val-129α_{TP}, Tyr-244α_{TP}, Leu-245α_{TP}, Tyr-248α_{TP} and Ala-19β_{TP} form hydrophobic–hydrophobic contacts in three out of four cases.

For Site II, composed entirely of α_{TP}-subunit residues, Thr-425α_{TP} is predicted to form a hydrogen bond with tentoxin in all ring conformations, while Val-367α_{TP}, Tyr-397α_{TP} and Arg-398α_{TP} will do so in three out of four cases (Table 3). The list of residues that form hydrophobic–hydrophobic contacts with tentoxin in all ring conformations (Leu-356α_{TP}, Ile-361α_{TP}, Val-367α_{TP}, Leu-394α_{TP}, Ala-401α_{TP}, Leu-428α_{TP}), or in three out of four cases (Ala-152α_{TP}, Ile-365α_{TP}, Tyr-397α_{TP}, Phe-403α_{TP}, Thr-425α_{TP}), is extensive (Table 3). In addition, LPC analysis indicates that Phe-403α_{TP} will also form aromatic–aromatic contacts with tentoxin in most complex conformations.

For Site III, there are two potential hydrogen bonds formed with tentoxin, both scoring positive in only two

out of the four ring conformations (Table 4). However, all of the ten putative, hydrophobic–hydrophobic contacts score positive for either four out of four or three out of four ring conformations (Table 4).

Discussion

Biological relevance of Sites I, II and III

In this study, we analysed the putative binding site(s) for tentoxin in plastid CF1-ATPase based on the structure of bovine mitochondrial F1-ATPase. Docking was to the whole volume of the crystallographic asymmetric unit of the unit cell ($\alpha_3\beta_3\gamma$), without any bias for a particular location. Currently, such docking procedures can readily result in several cavities with a similar level of complementarity and, indeed, this was the case in our study. Independent experimental data are, therefore, important for evaluating and deciding among the various possibilities.

Site I includes residue Glu-67β_{TP}, which corresponds to Glu-83β in plastid CF1-ATPase (cf., Figure 3 b). Avni et al.[17] proved, and others have since confirmed[18,19], the molecular–genetic importance of this residue in the inhibitory, high-affinity response of CF1 to tentoxin. Moreover, tentoxin is a non-competitive inhibitor of photophosphorylation[9]; thus, the high-affinity site should be located out of the catalytic nucleotide-binding site. Indeed, Glu-67β_{TP} is situated in the crown region of the β-subunit, spatially distinct from the catalytic site[23]. Aside from 67β_{TP} in Site I, whose phylogenetic amino acid composition was previously used to distinguish between tentoxin resistance and sensitivity[17], we do not find another residue at any of the three binding sites described here, that readily distinguishes between toxin sensitivity and resistance.

Not surprisingly, several studies have used codon 83β as a starting point in an attempt to derive the composition of the high-affinity tentoxin site. Based on the structure of bovine mitochondrial F1-ATPase, Santolini et al.[14]

a α-Subunits

```
CHL  MAMRTPEELSNLIKDLIEQYTPEVKMVDFGIVFQVGDGIARIYGLEKAMSGELLEFEDGT  60
MIT   EKTGTAEVSSILEERILGADTSVDLEETGRVLSIGDGIARVHGLRNVQAEEMVEFSSGL  59

CHL  LGIALNLEANNVGAVLLGDGLKITEGSRVRCTGKIAEIPVGEAYLGRVVDGLARPVDGKG  120
MIT  KGMSLNLEPDNVGVVVFGNDKLIKEGDIVKRTGAIVDVPVGEELLGRVVDALGNAIDGKG  119

CHL  AVQTKDSRAIESPAPGIVARRSVYEPLATGLVAVDAMIPVGRGQRELIIGDRQTGKTAIA  180
MIT  PIGSKARRRVGLKAPGIIPRISVREPMQTGIKAVDSLVPIGRGQRELIIGDRQTGKTSIA  179

CHL  VDTILNQK........GKGVICVYVAIGQKASSVAQVLNTLKERGALDYTIIVMANANEP  232
MIT  IDTIINQKRFNDGTDEKKKLYCIYVAIGQKRSTVAQLVKRLTDADAMKYTIVVSATASDA  239

CHL  ATLQYLAPYTGATLAEYFMYTGRPTLTIYDDLSKQAQAYREMSLLLRRPPGREAYPGDVF  292
MIT  APLQYLAPYSGCSMGEYFRDNGKHALIIYDDLSKQAVAYRQMSLLLRRPPGREAYPGDVF  299

CHL  YLHSRLLERAAKLNNALGEGSMTALPIVETQEGDVSAYIPTNVISITDGQIFLAAGLFNS  352
MIT  YLHSRLLERAAKMNDAFGGGSLTALPVIETQAGDVSAYIPTNVISITDGQIFLETELFYK  359

CHL  GLRPAINVGISVSRVGSAAQPKAMKQVAGKLKLELAQFAELEAFSQFASDLDQATQNQLA  412
MIT  GIRPAINVGLSVSRVGSAAQTRAMKQVAGTMKLELAQYREVAAFAQFGSDLDAATQQLLS  419

CHL  RGARLREILKQPQSSPLSVEEQVASLYAGTNGYLDKLEVSQVRAYLSGLRSYLANSYPKY  472
MIT  RGVRLTELLKQGQYSPMAIEEQVAVIYAGVRGYLDKLEPSKITKFENAFLSHVISQHQAL  479

CHL  GEILRSTLTFTPEAEGLVKQAINEYLEEFKSQAKAA                          508
MIT  LGKIRTDGKISEESDAKLKEIVTNFLAGFEA                               510
```

Figure 3 a. Alignment of CF1- and F1-ATPase sequences from *Chlamydomonas reinhardtii* chloroplasts (CHL) and bovine heart mitochondria (MIT). Numbering for CHL sequences as in SwissProt (accession numbers P26526, P06541, P12113). Numbering for MIT sequences as in the ATOM section of PDB file 1bmf. Site I residues are highlighted in yellow, Site II residues in cyan and Site III residues in green. The ANP (adenylyl-imidodiphosphate)-binding site residues at the α_{TP}/β_E interface[23] are underscored in red.

b β-Subunits

```
CHL   MPWGILIPLTMSDSIETKNMGRIVQIIGPVLDIVFAKGQVPNIYNALTIRAKNSAGTEMA 60
MIT         AAQASPSPKAGATTGRIVAVIGAVVDVQFDEG.LPPILNALEVQGR.....ETR 44


CHL   VTCEVQQLLGDNCVRAVSMNPTEGLMRGMEVVDTGKPLSVPVGKVTLGRIFNVLGEPVDN 120
MIT   LVLEVAQHLGESTVRTIAMDGTEGLVRGQKVLDSGAPIRIPVGPETLGRIMNVIGEPIDE 104


CHL   MGNVKVEETLPIHRTAPAFVDLDTRLSIFETGIKVVDLLAPYRRGGKIGLFGGAGVGKTV 180
MIT   RGPIKTKQFAAIHAEAPEFVEMSVEQEILVTGIKVVDLLAPYAKGGKIGLFGGAGVGKTV 164


CHL   LIMELINNIAKAHGGVSVFAGVGERTREGNDLYTEMKESGVIVEKNLSDSKVALVYGQMN 240
MIT   LIMELINNVAKAHGGYSVFAGVGERTREGNDLYHEMIESGVINLKD.ATSKVALVYGQMN 223


CHL   EPPGARMRVALTALTMAEYFRDVNKQDVLFFIDNIFRFVQAGAEVSALLGRMPSAVGYQP 300
MIT   EPPGARARVALTGLTVAEYFRDQEGQDVLLFIDNIFRFTQAGSEVSALLGRIPSAVGYQP 283


CHL   TLATEMGGLQERITSTKDGSITSIQAVYVPADDLTDPAPATTFAHLDATTVLSRNLAAKG 360
MIT   TLATDMGTMQERITTTKKGSITSVQAIYVPADDLTDPAPATTFAHLDATTVLSRAIAELG 343


CHL   IYPAVDPLESTSTMLQPWILGEKHYDSAQSVKKTLQRYKELQDIIAILGLDELSEEDRLI 420
MIT   IYPAVDPLDSTSRIMDPNIVGSEHYDVARGVQKILQDYKSLQDIIAILGMDELSEEDKLT 403


CHL   VARARKIERFLSQPFFVAEVFTGSPGKYVSLAETIEGFGKIFAGELDDLPEQAFYLVGNI 480
MIT   VSRARKIQRFLSQPFQVAEVFTGHLGKLVPLKETIKGFQQILAGEYDHLPEQAFYMVGPI 463


CHL   TEAISKAASLK                                                 491
MIT   EEAVAKADKLA                                                 474
```

c γ-Subunits

```
CHL   MAAMLASKQGAFMGRSSFAPAPKGVASRGSLQVVAGLKEVRDRIASVKNTQKITDAMKLV 60
MIT                                         ATLKDITRRLKSIKNIQKITKSMKMV 26


CHL   AAAKVRRAQEAVVNGRPFSENLVKVLYGVNQRVRQEDVDSPLCAVRPVKSVLLVVLTGDR 120
MIT   AAAKYARAERELKPARVYGVGSLALYEKADIKT...........PEDKKKHLIIGVSSDR 75


CHL   GLCGGYNNFIIKKTEARYRELTAMGVKVNLVCVGRKGAQYFARRKQYNIVKSFSLGAA.. 178
MIT   GLCGAIHSSVAKQMKSEAANLAAAGKEVKIIGVGDKIRSILHRTHSDQFLVTFKEVGRRP 135
200
CHL   PSTKEAQGIADEIFASFIAQESDKVELVFTKFISLINSNPTIQTLLPMTPMGELCDVDGK 238
MIT   PTFGDASVIALELLNS..GYEFDEGSIIFNRFRSVISYKTEEKPIFSLDTISS....... 186


CHL   CVDAADDEIFKLTTKGGEFAVEREKTTIETEALDPSLIFEQEPAQILDALLPLYMSSCLL 298
MIT   ...............................AESMSIYDDIDADVLRNYQEYSLANIIY 214


CHL   RSLQEALASELAARMNAMNNASDNAKELKKGLTVQYNKQRQAKITQELAEIVGGAAATSG 358
MIT   YSLKESTTSEQSARMTAMDNASKNASEMIDKLTLTFNRTRQAVITKELIEIISGAAAL   272
```

Figure 3 *b*, *c*. Alignment of CF1- and F1-ATPase sequences from *Chlamydomonas reinhardtii* chloroplasts (CHL) and bovine heart mitochondria (MIT). Numbering for CHL sequences as in SwissProt (accession numbers P26526, P06541, P12113). Numbering for MIT sequences as in the ATOM section of PDB file 1bmf. Site I residues are highlighted in yellow and Site III residues in green. The ANP (adenylyl-imidodiphosphate)-binding site residues at the α_{TP}/β_E interface[23] are underscored in red. The DELSEED motif in the β-subunit[37] is underlined in purple.

Table 3. Site II residues at the α$_{TP}$-subunit forming potential hydrogen bonds or hydrophobic contacts with tentoxin

Bovine mitochondria	Tentoxin ring conformation[a]				Chlamydomonas chloroplast[b]
	A	B	C	D	
Potential hydrogen bonds					
Val-367	+	–	+	+	Val-360
Gly-368	–	+	+	–	Gly-361
Tyr-397	–	+	+	+	Phe-390
Arg-398	+	+	+	–	Ala-391
Thr-425	+	+	+	+	Arg-418
Potential hydrophobic contacts					
Ala-152	+	+	–	+	Ala-153
Leu-156	–	+	+	–	Met-157
Leu-356	+	+	+	+	Leu-349
Ile-361	+	+	+	+	Leu-354
Ile-365	+	+	–	+	Ile-358
Val-367	+	+	+	+	Val-360
Leu-394	+	+	+	+	Leu-387
Tyr-397	+	–	+	+	Phe-390
Ala-401	+	+	+	+	Glu-394
Phe-403	+	+	+	–	Phe-396
Thr-425	+	+	–	+	Arg-418
Leu-428	+	+	+	+	Leu-421

[a]See comment in Table 2.
[b]As aligned in Figure 3 *a*.

Table 4. Site III residues at the α$_{TP}$/β$_E$/γ interface forming potential hydrogen bonds or hydrophobic contacts with tentoxin

Bovine mitochondria	Subunit	Tentoxin ring conformation[a]				Chlamydomonas chloroplast[b]
		A	B	C	D	
Potential hydrogen bonds						
Lys-24	γ	–	–	+	+	Lys-58
Tyr-31	γ	+	+	–	–	Val-65
Potential hydrophobic contacts						
Phe-406	α$_{TP}$	+	+	+	+	Phe-399
Ile-387	β$_E$	+	+	+	+	Ile-404
Ile-390	β$_E$	+	–	+	+	Ile-407
Leu-391	β$_E$	+	+	+	+	Leu-408
Met-25	γ	+	–	+	+	Leu-59
Ala-28	γ	+	+	+	+	Ala-62
Tyr-31	γ	+	+	+	+	Val-65
Ala-32	γ	+	+	–	+	Arg-66
Met-229	γ	+	+	+	+	Met-313
Thr-230	γ	+	+	+	–	Asn-314

[a]See comment in Table 2.
[b]As aligned in Figure 3 *a–c*.

suggested the involvement of α$_{TP}$- and β$_{TP}$-subunits and residue Tyr-300α$_{TP}$ in the inhibitory binding site. Groth and Pohl[26] and Tucker *et al.*[19,20] assumed codon 83β as the centre of the binding pocket. Residues at a radius of 10 Å from 83β were taken as putative residues forming the inhibitory, high-affinity tentoxin-binding site. However, residue 83β is located at a wall, not the centre, of the cavity. We calculated the distance between the average geometric centre of docked tentoxin in Site I (considering rings A–D) and the Cα atom of residue Glu-67β$_{TP}$

(codon 83β in CF1), and found it to be > 8 Å. Thus, Site I in our study and the binding site suggested by Groth and Pohl[26] and Tucker *et al.*[19,20] are displaced by almost an entire cavity radius. Although both sites include approximately the same number of residues (32 in our study and 31 in Groth and Pohl[26]), only 16 residues overlap (cf., Figure 1 *e*). Correspondingly, a number of Site I residues are more than 10 Å from codon 83β, while several residues listed by Groth and Pohl[26] are located in the protein core and have solvent-accessible surfaces equal to zero.

The full set of 32 residues forming Site I (cf., Figure 1) was obtained by summarizing all residues in contact with tentoxin at least once in the 22 structures docked at this site. However, for any given conformation, tentoxin is in contact with only a subset of these. A number of residues are common to all four ring structures (Figure 1 *e*) and these are prime candidates for molecular–genetic manipulation. On the other hand, manipulation of residues not in direct contact with the ligand in a given conformation (those coloured green in Figure 1 *a–d*) may enable subtle changes in cavity structure. Mutation of such residues is unlikely to dramatically affect the protein structure, as they are situated at the cavity surface and not in the protein core.

Based on early experimental data discussed in Pick *et al.*[11], the low-affinity binding site of tentoxin was postulated to be close to the nucleotide-binding sites. Indeed, recent analysis of the kinetics of tentoxin-binding furnishes strong evidence for an interaction between the low-affinity site and the nucleotide-binding ones[14]. The location of putative Site II in this study (cf., Figure 2) is compatible with this description. Analysis of the 1bmf $\alpha_3\beta_3\gamma$ structure shows that Site II has a residue (Pro-363α_{TP}) in common with the nucleotide-binding pocket of the α_{TP}-subunit (Figure 3 *a*).

Biological input exists as well for putative Site III. This site overlaps with residues forming an energy-coupling region between γ- and β-subunits in F1-ATPase. Site III residue Glu-395β$_E$ (corresponding to Glu-412β$_E$ in CF1) is in the conserved sequence motif DELSEED[37] (Figure 3 *b*). Also, Site III residue Lys-24γ (corresponding to Lys-58γ in CF1) is the nearest neighbour to Met-23γ, a residue that plays a key role in energy coupling[37], although not rotation[38,39] of F1-ATPase. It has been established that high concentrations of tentoxin lead to over-energization of the thylakoid membrane, possibly through interaction with a tentoxin low-affinity binding site[40]. Thus, Site III also potentially satisfies the requirement of a low-affinity site. As opposed to Sites I and II, which are embedded pockets, Site III is partially surface-exposed and has positional potential for interaction with other macromolecular components, particularly the δ- and ε-subunits (and unresolved sections of γ) of F1 itself. However, our visual analysis of the detailed structure of the central stalk in bovine F1-ATPase[5] indicates that Site III is indeed a surface-exposed niche in which tentoxin can potentially be situated.

Sites I–III and rotation of the γ-subunit

There is no direct structural evidence as to how tentoxin binding influences ATPase function. One may speculate[9,12] that flexibility of the Site I region is important for function and that by binding, tentoxin freezes this region, possibly by restricting conformational mobility in a manner similar to that suggested for efrapeptin in inhibiting F1-ATPase[3,41]. Considerable experimental data support the rotation of the γ-subunit during ATPase function[33,36,42]. The question arises: does tentoxin affect function by interfering with γ rotation? It has been shown that tentoxin does not inhibit $\alpha_3\beta_3$ functions in the absence of the γ-subunit[41]. Our study shows that Site I residues are not in direct contact with the γ-subunit. However, we can identify several residues dually contacting both the Site I pocket and γ-subunit. Thus, blockage at Site I is structurally feasible. We have shown that Site II peripherally overlaps with the α-subunit nucleotide-binding site, and Site III with the γ-subunit (at residues distinct from those interacting with the β-DELSEED sequence; compare Hara *et al.*[38] and Figure 3 *c*). Thus, blockage at these sites is potentially feasible as well. Theoretical arguments notwithstanding, the actual relationship, if any, of tentoxin binding to γ-subunit rotation needs to be clarified by mutational studies. As some of the hypothetical sites are in the vicinity of regions that play crucial roles in catalysis, only mutations not affecting these activities can be tested.

Materials and methods

F1-ATPase structures analysed

PDB file 1cow (ref. 2) was used for cavity searching and 1bmf (ref. 23) for docking. Following Abrahams *et al.*[23] the seven peptide chains in these crystals are referred to as α_E, α_{TP}, α_{DP}, β_{DP}, β_E, β_{TP} and γ.

Numbering of F1 and CF1 residues

Unless otherwise indicated, all numbering of F1 residues is as in the ATOM section of PDB file 1bmf. Numbering of CF1 residues in the α-, β- and γ-subunits is as in SwissProt, accession numbers P26526, P06541 and P12113 respectively.

Docking procedure

LIGIN software for molecular docking[30] was used for predicting the position of tentoxin within a putative binding site. The program generates a number of randomly distributed ligand positions within the putative binding site and maximizes complementarity as a function of the

six degrees of freedom of the ligand[43]. Density of starting points was kept at > 4 points per Å^3. Multiple ligand conformations were docked; however, during the optimization procedure, ligand and protein were treated as rigid bodies.

Ligand flexibility

A schematic representation of tentoxin is shown in Figure 4. The cyclic tetrapeptide ring has a *cis–trans–cis–trans* conformation, both in chloroform[44] and water[45]. In chloroform, one conformer (B-form) of the ring predominates; however, in aqueous solutions there are four forms – A, B, C and D, in relative proportions 51:37:8:4 respectively[45]. We incorporated ligand flexibility in our docking procedure to allow for any of several conformers of tentoxin. The rationale was that from many ligand conformers in solution, the apoprotein most likely selects one with high complementarity to the binding site. We considered all four forms of the ring. To determine the structure of forms A and B, the backbone torsion angles given in Pinet *et al.*[45] were used. We created the C and D structures from the B-form; by adding 180° to Φ_{Gly} and Ψ_{Phe} to obtain C, and by flipping the two non-methylate peptidic bond planes to obtain D. The structures were then refined by energy minimization[46] using AMBER force field[47].

We also considered the different side-chain orientations for ΔPhe (dehydrophenylalanyl) and Leu. In tentoxin, ΔPhe almost exclusively assumes a Z-configuration[48]. However, at equilibrium ∼3% of molecules can exist in the E-configuration as isotentoxin. Moreover, the C-conformation of a synthetic analogue of tentoxin, MeSer[1]-tentoxin, takes the E-configuration[49]. Although it

is not yet clear whether the E-conformation is relevant *in vivo*[50], we decided not to exclude it a priori, and considered both configurations of ΔPhe in our preliminary calculations. As for Leu, its side chain has two rotatable bonds with three rotamers per bond. We considered all Leu rotamers that did not produce atomic bumping. *In toto*, 44 tentoxin conformations were initially applied in the docking procedure. Since the results for the E- and Z-conformations were similar, we present only data corresponding to binding complementarity of the 22 conformations of the latter. This number of conformations is readily managed by our docking procedure. Data for the 22 tentoxin conformations are presented at the website htpp://sgedg.weizmann.ac.il/tentoxin/

Analytical tools

Complementarity, a geometric and chemical measure of ligand–protein fitness[30], was used to gauge complex stability. LPC and CSU software[22] were used to determine the interactions stabilizing the structures obtained. Tentoxin has four ring conformations: A, B, C and D (ref. 45). For each ring conformation, LPC analysis was performed for the complex structure with the highest complementarity.
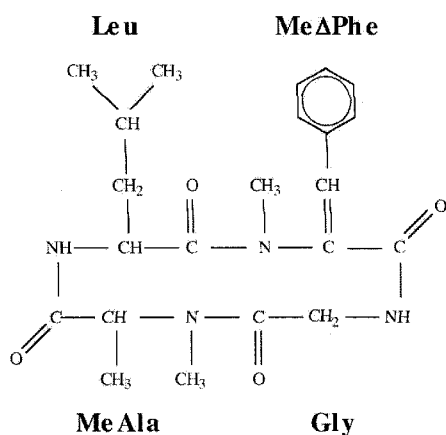

Figure 4. Schematic representation of tentoxin: cyclo-[L-leucyl-N-methyl-(Z)-dehydrophenylalanyl-glycyl-N-methyl-alanyl]. Component residues are indicated. Tentoxin flexibility involves the four main conformations of the backbone ring, two configurations of the MeΔPhe double bond and rotation around the two single bonds of the Leu side chain (see text for details).

1. McCarty, R. E., in *Oxygenic Photosynthesis: The Light Reaction* (eds Ort, D. R. and Yocum, C. F.), Kluwer, Dordrecht, 1996, pp. 439–451.
2. Van Raaij, M. J., Abrahams, J. P., Leslie, A. G. W. and Walker, J. E., *Proc. Natl. Acad. Sci. USA*, 1996, **93**, 6913–6917.
3. Abrahams, J. P., Buchanan, S. K., Van Raaij, M. J., Fearnley, I. M., Leslie, A. G. W. and Walker, J. E., *ibid*, 1996, **93**, 9420–9424.
4. Orriss, G. L., Leslie, A. G. W., Braig, K. and Walker, J. E., *Structure*, 1998, **6**, 831–837.
5. Gibbons, C., Montgomery, M. G., Leslie, A. G. W. and Walker, J. E., *Nature Struct. Biol.*, 2000, **7**, 1055–1061.
6. Meyer, W. L., Templeton, G. E., Grable, C. I., Sigel, C. W., Jones, R., Woodhead, S. H. and Sauer, C., *Tetrahedron Lett.*, 1971, **25**, 2357–2360.
7. Steele, J. A., Uchytil, T. F., Durbin, R. D., Bhatnagar, P. and Rich, D. H., *Proc. Natl. Acad. Sci. USA*, 1976, **73**, 2245–2248.
8. Durbin, R. D. and Uchytil, T. F., *Phytopathology*, 1977, **67**, 602–603.
9. Dahse, I., Pezennec, S., Girault, G., Berger, G., Andre, F. and Liebermann, B., *J. Plant Physiol.*, 1994, **143**, 615–620.
10. Arntzen, C. J., *Biochim. Biophys. Acta*, 1972, **283**, 539–542.
11. Pick, U., Conrad, P. L., Conrad, J. M., Durbin, R. D. and Selman, B. R., *ibid*, 1982, **682**, 55–58.
12. Fromme, P., Dahse, I. and Graber, P., *Z. Naturforsch.*, 1992, **C47**, 239–244.
13. Santolini, J., Haraux, F., Sigalat, C., Munier, L. and Andre, F., *J. Biol. Chem.*, 1998, **273**, 3343–3350.
14. Santolini, J., Haraux, F., Sigalat, C., Moal, G. and Andre, F., *ibid*, 1999, **274**, 849–858.
15. Mochimaru, M. and Sakurai, H., *FEBS Lett.*, 1997, **419**, 23–26.
16. Steele, J. A., Durbin, R. D., Uchytil, T. F. and Rich, D. H., *Biochim. Biophys. Acta*, 1978, **501**, 72–82.

17. Avni, A., Anderson, J. D., Holland, N., Rochaix, J.-D., Gromet-Elhanan, Z. and Edelman, M., *Science*, 1992, **257**, 1245–1247.
18. Hu, D., Fiedler, H. R., Golan, T., Edelman, M., Strotmann, H., Shavit, N. and Leu, S., *J. Biol. Chem.*, 1997, **272**, 5457–5463.
19. Tucker, W. C., Du, Z., Hein, R., Richter, M. L. and Gromet-Elchanan, Z., *ibid*, 2000, **275**, 906–912.
20. Tucker, W. C., Du, Z. Y., Hein, R., Gromet-Elchanan, Z. and Richter, M. L., *Biochemistry*, 2001, **40**, 7542–7548.
21. Bernstein, F. C. *et al.*, *J. Mol. Biol.*, 1997, **112**, 535–542.
22. Sobolev, V., Sorokine, A., Prilusky, J., Abola, E. E. and Edelman, M., *Bioinformatics*, 1999, **15**, 327–332.
23. Abrahams, J. P., Leslie, A. G. W., Lutter, R. and Walker, J. E., *Nature*, 1994, **370**, 621–628.
24. Bianchet, M. A., Hullihen, J., Pedersen, P. L. and Amzel, L. M., *Proc. Natl. Acad. Sci. USA*, 1998, **95**, 11065–11070.
25. Shirakihara, Y. *et al.*, *Structure*, 1997, **5**, 825–836.
26. Groth, G. and Pohl, E., *J. Biol. Chem.*, 2001, **276**, 1345–1352.
27. Altschul, S. F., Madden, T. L., Schaffer, A. A., Zhang, J. H., Zhang, Z., Miller, W. and Lipman, D. J., *Nucleic Acids Res.*, 1997, **25**, 3389–3402.
28. Groth, G., *Proc. Natl. Acad. Sci. USA*, 2002, **99**, 3464–3468.
29. Rich, D. H. and Bhatnagar, P. K., *J. Am. Chem. Soc.*, 1978, **100**, 2212–2218.
30. Sobolev, V., Wade, R. C., Vriend, G. and Edelman, M., *Proteins*, 1996, **25**, 120–129.
31. Walker, J. E., Saraste, M., Runswick, M. J. and Gay, N. J., *EMBO J.*, 1982, **1**, 945–951.
32. Boyer, P. D., *Biochim. Biophys. Acta*, 1993, **1140**, 215–240.
33. Noji, H., Yasuda, R., Yoshida, M. and Kinosita, K. Jr., *Nature*, 1997, **386**, 299–302.
34. Sabbert, D., Engelbrecht, S. and Junge, W., *ibid*, 1996, **381**, 623–625.
35. Wang, H. and Oster, G., *ibid*, 1998, **396**, 279–282.
36. Yasuda, R., Noji, H., Yoshida, M., Kinoshita, K. and Itoh, H., *ibid*, 2001, **410**, 898–904.
37. Ketchum, C. J., Al-Shawi, M. K. and Nakamoto, R. K., *Biochem. J.*, 1998, **330**, 707–712.
38. Hara, K. Y., Noji, H., Bald, D., Yasuda, R., Kinosita, K. Jr. and Yoshida, M., *J. Biol. Chem.*, 2000, **275**, 14260–14263.
39. Hara, K. Y., Kato-Yamada, Y., Kikuchi, Y., Hisabori, T. and Yoshida, M., *ibid*, 2001, **276**, 23969–23973.
40. Holland, N., Evron, Y., Jansen, M. A. K., Edelman, M. and Pick, U., *Plant Physiol.*, 1997, **114**, 889–892.
41. Sokolov, M. and Gromet-Elhanan, Z., *Biochemistry*, 1996, **35**, 1242–1248.
42. Yasuda, R., Noji, H., Kinosita, K. Jr. and Yoshida, M., *Cell*, 1998, **93**, 1117–1124.
43. Sobolev, V. and Edelman, M., *Proteins*, 1995, **21**, 214–225.
44. Rich, D. H. and Bhatnagar, P. K., *J. Am. Chem. Soc.*, 1978, **100**, 2218–2224.
45. Pinet, E., Neumann, J.-M., Dahse, I., Girault, G. and Andre, F., *Biopolymers*, 1995, **36**, 135–152.
46. Mohamadi, F. *et al.*, *J. Comp. Chem.*, 1990, **11**, 440–467.
47. Weiner, S. J. *et al.*, *J. Am. Chem. Soc.*, 1984, **106**, 765–784.
48. Bland, J. M., Edwards, J. V., Eaton, S. R. and Lax, A. R., *Pestic. Sci.*, 1993, **39**, 331–340.
49. Pinet, E. *et al.*, *Biochemistry*, 1996, **35**, 12804–12811.
50. Liebermann, B., Ellinger, R. and Pinet, E., *Phytochemistry*, 1996, **42**, 1537–1540.